

## Magnetorotational Instability in Magnetized Couette Flow

Hantao Ji<sup>1\*</sup>, Jeremy Goodman<sup>2</sup>, and Akira Kageyama<sup>1,3</sup>

<sup>1</sup> Princeton Plasma Physics Laboratory, Princeton University, P.O. Box 451, Princeton, NJ 08543, USA

<sup>2</sup> Princeton University Observatory, Peyton Hall, Princeton, NJ 08544, USA

<sup>3</sup> National Institute for Fusion Science, Oroshi-cho, Toki, 509-5292, Japan

\* Corresponding author: Hantao Ji, hji@pppl.gov

### Abstract

Axisymmetric stability of magnetized Couette flow is revisited in an attempt to demonstrate and study the magnetorotational instability (MRI) in the laboratory. The MRI has been widely accepted as a powerful accretion mechanism in magnetized accretion disks. Stability diagrams are drawn in dimensionless parameters, and also in terms of the angular velocities at the inner and outer cylinders. It is shown that MRI can be triggered in a moderately rapidly rotating table-top apparatus, using easy-to-handle metals such as gallium. Practical issues of this proposed experiment are discussed.

### Introduction

Rapid angular momentum transport in accretion disks has been a longstanding astrophysical puzzle [1]. The molecular viscosity of astrophysical gases and plasmas is completely inadequate to explain observationally inferred accretion rates, so that a turbulent viscosity is required. Recent theoretical work indicates that purely hydrodynamic instabilities are absent or ineffective, but that magnetorotational instabilities (MRI) [2–4] are robust and support vigorous turbulence in electrically-conducting disks. It is now believed [5] that MRI drives accretion in disks ranging from quasars and X-ray binaries to cataclysmic variables and perhaps even protoplanetary disks. Despite much theoretical and computational work, however, MRI has never been demonstrated in the laboratory. Past work on the magnetized Couette flow using liquid metals [6–9] has focused on magnetic stabilization of the Rayleigh instability, as first analyzed by Chandrasekhar [10]. This paper summarizes theoretical and numerical work to predict requirements to realize MRI in a magnetized Couette flow.

### Local and Global Stability Analysis

Linear stability analysis has been performed in order to explore the possibilities of MRI in a magnetized Couette flow using liquid metals. The dimensions of the flow are determined by its height ( $h$ ), inner and outer radius ( $r_1, r_2$ ). The flow dynamics are governed by the incompressible and dissipative magnetohydrodynamic (MHD) equations including both resistivity,  $\eta$ , and viscosity,  $\nu$ . The flow is driven by rotating the inner and outer cylinders at  $\Omega_1$  and  $\Omega_2$ , respectively. A uniform magnetic field  $B$  is imposed along the axial direction,  $z$ , in cylindrical coordinates  $(r, \theta, z)$ .

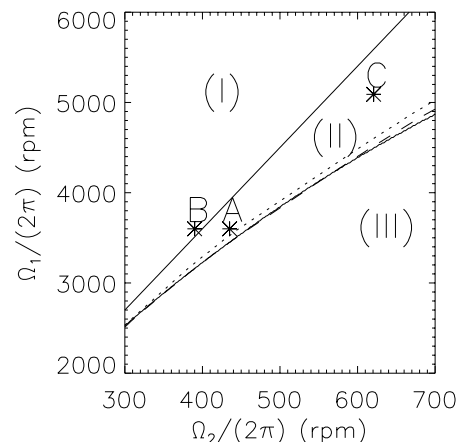


FIG. 1. Stability diagram in the  $(\Omega_1, \Omega_2)$  space using liquid gallium and  $r_1=0.05\text{m}$ ,  $r_2=0.15\text{m}$ , and  $h=0.1\text{m}$ . Here the stability can be divided into 3 regions: region (I) is hydrodynamically unstable but can be stabilized by a large enough magnetic field, as exemplified by point B. Region (II) is hydrodynamically stable but can be destabilized by presence of a magnetic field (MRI), as exemplified by points A and C. Region (III) is always stable. Results from global eigenmode analysis are also shown: dotted lines for conducting boundary conditions and dashed lines for insulating boundary conditions.

In the local WKB approximation, all perturbations are assumed to be proportional to  $\exp(\gamma t - ik_z z - ik_r r)$  where  $\gamma$  is the growth rate and the minimum  $k_z$  and  $k_r$  are given by  $\pi/h$  and  $\pi/(r_2 - r_1)$ , respectively. The total wavenumber  $k$  is given by  $\sqrt{k_z^2 + k_r^2} = k_z \sqrt{1 + \epsilon^2}$ , where  $\epsilon \equiv h/(r_2 - r_1)$ . The dispersion relation of axisymmetric perturbations is given by [11]

$$\begin{aligned}
 & [(\gamma + \nu k^2)(\gamma + \eta k^2) + (k_z V_A)^2] \frac{k^2}{k_z^2} + \kappa^2 (\gamma + \eta k^2)^2 \\
 & + \frac{\partial \Omega^2}{\partial \ln r} (k_z V_A)^2 = 0, \quad (1)
 \end{aligned}$$

where the epicyclic frequency is defined by  $\kappa^2 \equiv (1/r^3)\partial(r^4\Omega^2)/\partial r = 4\Omega^2 + \partial\Omega^2/\partial \ln r$  and the Alfvén speed is  $V_A \equiv B/\sqrt{\mu_0\rho}$ . Note that this dispersion relation is identical to the one derived for accretion disks in the incompressible limit [12].

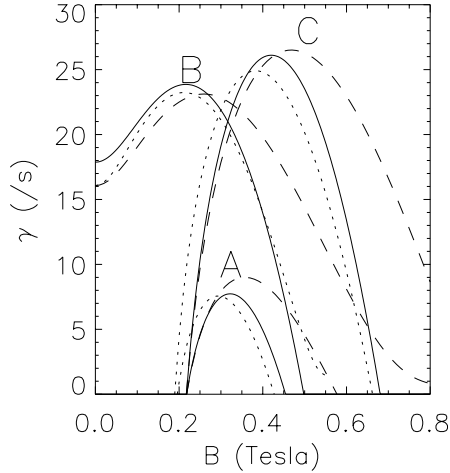


FIG. 2. The growth rates of points A, B, and C as functions of magnetic field. Results from global eigenmode analysis are also shown: dotted lines for conducting boundary conditions and dashed lines for insulating boundary conditions.

The stability diagram [11] in the  $(\Omega_1, \Omega_2)$  space is shown in Fig. 1 in the limit of small viscosity compared to resistivity in liquid gallium with  $h = 0.1\text{m}$ ,  $r_1 = 0.05\text{m}$ , and  $r_2 = 0.15\text{m}$ . The stability can be divided into three regions: region (I) is Rayleigh unstable but can be stabilized by a large enough magnetic field, as exemplified by point B. Region (II) is hydrodynamically stable but can be destabilized by presence of a magnetic field (MRI), as exemplified by points A and C. Region (III) is always stable. Figure 2 shows growth rates as functions of magnetic field. It can be seen that the curves A and C represent MRI, which is triggered by an appropriate strength of the imposed magnetic field. Stability at both zero and infinite magnetic field is the hallmark of MRI [4,5].

The local WKB is a short-wavelength approximation, yet for the experimental parameters contemplated above, the fastest-growing MRI modes are predicted to have wavelengths twice the gap width and cylinder height. It is not clear that the WKB dispersion relation is applicable to these modes, so we have performed a global linear stability analysis [13]. The eigenfunctions turn out to be very nonsinusoidal, especially in the velocities, and sensitive to boundary conditions. However, the growth rates agree remarkably well with the WKB predictions.

A linearized, finite-difference, implicit initial-value code has been written to discover the fastest-growing mode. The code deals stably with boundary layers and is capable of finding overstability: *i.e.*, a growing oscillation with complex eigenfrequency. In fact, all of the growing

modes were found to be non-oscillatory. Axisymmetry is assumed, and periodic vertical boundary conditions with periodicity length twice the cylinder height, so that the vertical velocity has nodes at both ends of the cylinder. The equations of motion are discretized on a radial grid. Radial boundaries are impenetrable, no-slip, and electrically are either perfectly insulating or perfectly conducting. Results of the global and WKB analyses are compared in Figs. 1 and 2. Figure 3 shows eigenmodes for the parameters of point C with  $B=0.3$  Tesla. Differences between the conducting and insulating cases can be seen near the inner boundaries. A Hartmann layer [14], consisting of large toroidal and axial velocities within a radial thickness of  $\sim \sqrt{\nu\eta}/V_A$ , forms at the inner conducting boundary as the Lorentz force balances with the viscous force. Nevertheless, the growth rates are remarkably similar to those of the local analysis, which therefore should suffice for preliminary experimental design.

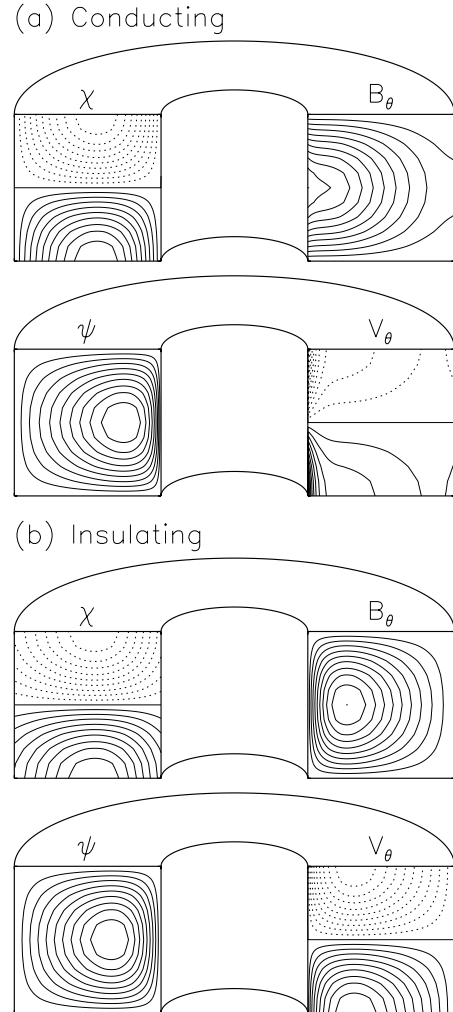


FIG. 3. Eigenmodes for conditions given by point C in Figs. 1 and 2 at  $B = 0.3$  Tesla with conducting (a) and insulating (b) radial boundaries. Here, solid (dotted) lines represent positive (negative) values;  $\chi$  and  $\psi$  are poloidal flux and stream functions, respectively.

## Linear and Nonlinear MHD Simulations

A fully nonlinear incompressible MHD code has been developed to study the problem in three dimensions. The fluid velocity and magnetic field are expanded in Chebyshev polynomials in the  $r$  direction. Chebyshev expansion is preferred since its nodes cluster near the inner and outer boundaries where boundary layers appear. Fourier expansions are used in the  $\theta$  and  $z$  directions. Chebyshev transformations between real and spectral space are swiftly performed at every time step by the fast cosine transformation. For the temporal integration of the MHD equation, we follow a time splitting method [15].

Initial results from linear and two-dimensional (axisymmetric) runs of this code with conducting, freely-slipping boundary conditions agree with the local and global analyses. For example, for the conditions given by the point C in Figs. 1 and 2 at  $B = 0.3$  Tesla, the growth rate is  $21.67 \text{ s}^{-1}$  from simulations,  $21.90 \text{ s}^{-1}$  from global analysis, and  $19.10 \text{ s}^{-1}$  from local analysis.

## Discussions and Conclusions

Several issues must be explored before committing to an experimental design. The first is geometric optimization with regard to aspect ratio [ $A \equiv (r_2 + r_1)/(r_2 - r_1)$ ] and elongation [ $\epsilon \equiv h/(r_2 - r_1)$ ]. Obviously,  $\epsilon \sim 1$  is desirable to minimize volume, and therefore expense, at a given growth rate. Less obviously, aspect ratios close to unity cause the eigenmodes and growth rates to be dominated by the inner cylinder. Therefore, moderate values of  $A$  ( $\sim 2$ ) and  $\epsilon$  ( $\sim 1$ ) are preferred.

The periodic vertical boundary conditions used in all of our analyses take no account of viscous (Ekman) layers at the top and bottom of the flow. The thickness of the Ekman layer is estimated to be small ( $\sim 10^{-3} h$  at point C). Thus the Ekman circulation time ( $\sim 2\text{s}$ ) is much longer than a typical MRI growth time if we use the laminar value for the viscosity  $\nu$ ; turbulent boundary layers may produce much more rapid Ekman circulation. To explore these issues, prototype experiments using water are underway in conjunction with numerical simulations in 2D and 3D. To minimize the effect of Ekman layers, if necessary, one could increase  $\epsilon$ , use differentially rotating rings at the vertical boundaries, or modify the boundary layer by localized Lorentz forces [9].

A third issue is finite-amplitude or nonlinear hydrodynamical instability in Rayleigh-stable regimes. It has been argued that a rapid Couette flow can be nonlinearly unstable [16]. However, there are indications that such instabilities are caused by wall surface defects [17]. If so, they should depend on the amplitude of the initial perturbation and the strength of the angular-momentum gradient. This issue is also being studied using water-filled prototype experiments.

In summary, we have used linear stability analyses and MHD simulations to explore prospects for the magnetorotational instability in a magnetized Couette flow. We find

that MRI can be achieved in a moderately rapidly rotating apparatus using an easy-to-handle liquid metal such as gallium. Auxiliary experiments with water are underway both as a prototype and as a control to distinguish MRI from nonlinear hydrodynamic instabilities. If successful, this will be a rare example of an astrophysical process that can be studied in the laboratory.

- 
- [1] Shakura, N.I. and Sunyaev, R.A., 1973, "Black holes in binary systems. Observational appearance," *Astron. & Astrophys.*, 24:337.
  - [2] Velikhov, E. P., 1959, "Stability of an ideally conducting liquid flowing between cylinders rotating in a magnetic field," *Sov. Phys. JETP*, 36:995–998.
  - [3] Chandrasekhar, S., 1960, "The stability of non-dissipative Couette flow in hydromagnetics," *Proc. Nat. Acad. Sci.*, 46:253–257.
  - [4] Balbus, S. A. and Hawley, J. F., 1991, "A powerful local shear instability in weakly magnetized disks. I - Linear analysis," *Astrophys. J.*, 376:214–222.
  - [5] Balbus, S. A. and Hawley, J. F., 1998, "Instability, turbulence, and enhanced transport in accretion disks," *Rev. Mod. Phys.*, 70:1.
  - [6] Donnelly, R.J. and Ozima, M., 1960, "Hydromagnetic stability of flow between rotating cylinders," *Phys. Rev. Lett.*, 4:497–498.
  - [7] Donnelly, R.J. and Ozima, M., 1962, "Experiments on the stability of flow between rotating cylinders in the presence of magnetic field," *Proc. R. Soc. Lond. A*, 266:272–286.
  - [8] Donnelly, R.J. and Caldwell, D.R., 1964, "Experiments on the stability of hydromagnetic Couette flow," *J. Fluid Mech.*, 19:257–263.
  - [9] Brahme, A., 1970, "On the Hydromagnetic Stability of a Nonuniformly Rotating Fluid," *Physica Scripta*, 2:108–112.
  - [10] Chandrasekhar, S., 1961, "Hydrodynamic and Hydro-magnetic Stability," London, Oxford University Press.
  - [11] Ji, H., Goodman, J., and Kageyama, A., 2001, "Magnetorotational instability in a rotating liquid metal annulus," accepted for publication in *Mon. Not. R. Astr. Soc.* (astro-ph/0103226)
  - [12] Sano, T. and Miyama, S., 1999, "Magnetorotational instability in protoplanetary disks. I. On the global stability of weakly ionized disks with ohmic dissipation," *Astrophys. J.*, 515:776–786.
  - [13] Goodman, J. and Ji, H., 2001, "Magnetorotational instability of dissipative Couette flow," submitted to *J. Fluid Mech.* (astro-ph/0104206)
  - [14] Hartmann, J., 1937, "Hg-dynamics I," *Mat-Fys. Medd.*, 15:6.
  - [15] Marcus, P. S., 1984, "Simulation of Taylor-Couette flow 2. Numerical results for wavy-vortex flow with one traveling wave," *J. Fluid Mech.*, 146:65–113.
  - [16] Richard, D. and Zahn, J.-P., 1999, "Turbulence in differentially rotating flows: What can be learned from the Couette-Taylor experiment," *Astron. Astrophys.*, 347:734–738.
  - [17] Schultz-Grunow, F., 1959, "Zur stabilität der Couette-Strömung," *Z. angew. Math. Mech.*, 39:101.